A bandpass filter using the operational amplifier pole

2 authors:

A.M. Soliman
Cairo University
554 PUBLICATIONS   **10,037** CITATIONS

SEE PROFILE

Mahmoud Fawzy Wagdy
California State University, Long Beach
52 PUBLICATIONS   **666** CITATIONS

SEE PROFILE

Some of the authors of this publication are also working on these related projects:

Project   Fractional-order systems View project

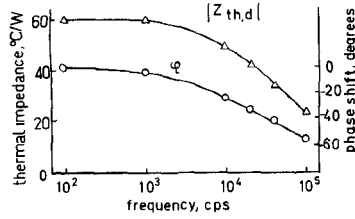Project   Self-Calibrating A/D Converters View project

Fig. 3. Temperature difference of the b-e junctions of Q_3 and Q_4 per watt of power change in the collector dissipation of Q_3 versus frequency.
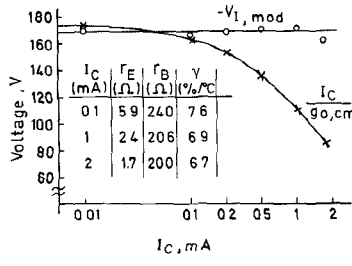

Fig. 4. The modified intercept voltage $V_{I, \text{mod}}$ of a CA3046 transistor versus the collector current. For comparison, the quotient I_C/g_o, cm of the current mirror is also represented.

$$g_{0,\text{cm}} = dI_{C3}/dV_{CE3} \simeq g_{0,\text{early}} + \gamma I_{C3}^2 R_{\text{th},d}, \tag{7}$$

where $R_{\text{th},d}$ represents the thermal differential resistance

$$R_{\text{th},d} \stackrel{\text{df}}{=} d(T_3 - T_4)/d(V_{CE3}I_{C3}). \tag{8}$$

The numerical subscripts correspond to those of the transistors. Analogously, for the long-tail pair [Fig. 2(b)], with short-circuited input terminals, it is found that the output conductance is half that of the current mirror.

The temperature difference $T_3 - T_4$, as a result of a power step in the collector dissipation of Q_3, is shown in the lower curve of Fig. 1. It can be seen that the slow effect is completely compensated for while the fast effect remains unchanged. For sinusoidal changes of the collector dissipation of Q_3 in (7), $R_{\text{th},d}$ is replaced by its corresponding complex value $Z_{\text{th},d}$ for which the curves of Fig. 3 are found.

RESULTS

The quotient of the collector current I_{C3} and the output conductance $g_{0,\text{cm}}$ of the current mirror is shown in Fig. 4 for various values of the bias current I_{C3}, as measured on a CA3046 array for low frequencies ($f < 10^3$ Hz) and a collector voltage $V_{CE} = 4$ V. The value of $g_{0,\text{cm}}$ is influenced by the emitter and base bulk resistances r_E and r_B, respectively. If these influences are accounted for, it can be found that

$$g_{0,\text{cm}} = \frac{I_C}{(1 + g_m r_E)(V_{CB} - V_I)} + \frac{\gamma I_C^2 R_{\text{th},d}}{1 + g_m \left(r_E + \dfrac{r_B}{\beta}\right)} \tag{9}$$

where $g_m = (\partial I_C/\partial V_{BE})|V_{CE} = qI_C/kT$ and β is the common-emitter current gain. Equation (9) holds also for the output conductance g_0 of a single transistor if for $R_{\text{th},d}$ the thermal impedance Z_{th} is substituted. In the inset in Fig. 4, some values of r_E and r_B are given as measured by Sansen and Meijer [4] for the electrically identical CA3045. The value of γ is determined according to (5). Using these parameters $V_{I, \text{mod}}$ is calculated from (9) and is represented in Fig. 4 versus the collector current. It is clear that the current depen-

dency of the quotient $I_{C3}/g_{0,\text{cm}}$ can be explained accurately by thermal feedback and the influence of the bulk resistance.

CONCLUSION

The current dependency of the output conductance of voltage-driven BJT's can be accurately described by (9) in which basewidth modulation, thermal feedback, and the bulk resistances are accounted for. The basewidth modulation can be characterized by a single current independent parameter V_I, mod. The thermal feedback is characterized by a parameter γ, and the thermal impedance Z_{th}.

This thermal impedance consists of a component depending on the transistor geometry and a component depending on the thermal properties of the package. The latter component is significant only for very low frequencies and is fully compensated for in certain transistor configurations widely used in IC's.

REFERENCES

[1] O. Mueller, "Internal thermal feedback in four-poles especially in transistors," Proc. IEEE, vol. 52, pp. 924-930, Aug. 1964.
[2] B. L. Hart and R. W. J. Barker, "Early-intercept voltage a parameter of voltage-driven B.J.T's," Electron. Lett., vol. 12, pp. 174-175, Apr. 1, 1976.
[3] J. W. Slotboom and H. C. de Graaff, "Measurements of bandgap narrowing in Si bipolar transistor," Solid-State Electron., vol. 19, pp. 857-862, Oct. 1976.
[4] W. M. C. Sansen and R. G. Meijer, "Characterization and measurement of the base and emitter resistances of bipolar transistors," IEEE J. Solid-State Circuits, vol. SC-7, pp. 492-498, Dec. 1972.

A Bandpass Filter Using the Operational Amplifier Pole

AHMED M. SOLIMAN AND MAHMOUD FAWZY

Abstract—The operational amplifier rolloff characteristics and a single capacitor are used for obtaining an inverting bandpass function. The filter performance depends on the gain-bandwidth product of the operational amplifier. Experimental results are included. The amplifier rolloff characteristics can be utilized in deriving transfer functions. The resulting filters have an extended frequency range of operation and a reduced number of external capacitors.

In this correspondence, the pole of an operational amplifier and a single capacitor are used to realize a second-order bandpass function. Taking [1]

$$A = \frac{GB}{s} \tag{1}$$

where GB is the gain-bandwidth product of the operational amplifier, we get for the circuit of Fig. 1

$$\frac{V_2}{V_1} = -\frac{sC \cdot R_1 \cdot R_2 \cdot GB}{s^2 CR_1 R_2 + s(R_1 + R_2) + R_1 GB}. \tag{2}$$

Equation (2) represents an inverting bandpass function with no cancellation term in the numerator, which is an advantage over the circuit of Rao and Srinivasan [2].
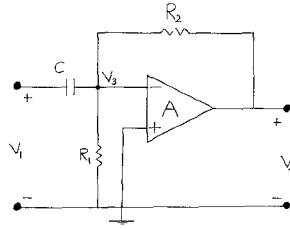
The bandpass performance factors are as follows:

Fig. 1. Inverting bandpass filter.

$$\omega_0 = \sqrt{\frac{GB}{CR_2}}, \quad Q = \frac{R_1}{R_1 + R_2}\sqrt{CR_2 \cdot GB},$$

$$G_0 = \frac{CR_1R_2}{R_1 + R_2} \cdot GB. \tag{3}$$

It is seen that

$$\omega_0 \cdot Q = GB \cdot \frac{R_1}{R_1 + R_2}. \tag{4}$$

For $R_1 = \infty$, a bandpass filter with one resistor and one capacitor is obtained which, when $A = \infty$, is a conventional differentiator circuit. The $\omega_0 \cdot Q$ product when $R_1 = \infty$ is double that of Rao and Srinivasan's circuit [2].

It is evident that since the filter performance depends critically on GB, a parameter that varies with temperature and supply voltage, no claim of stability can be made. This dependence on environmental and operating conditions, which is not avoided in our shown circuit, could be alleviated in a special design by using compensation schemes.

As far as GB is concerned, (3) has high variabilities since GB differs from one unit to another for the same operational amplifier type. That is why a precise determination of GB should precede the design process of a specific filter.

The ω_0 and Q sensitivities to all circuit parameters are given by

$$S_{GB}^{\omega_0} = 0.5, \quad S_C^{\omega_0} = -0.5, \quad S_{R_1}^{\omega_0} = 0, \quad S_{R_2}^{\omega_0} = -0.5$$

$$S_{GB}^Q = 0.5, \quad S_C^Q = 0.5, \quad S_{R_1}^Q = \frac{R_2}{R_1 + R_2},$$

$$S_{R_2}^Q = 0.5\frac{R_1 - R_2}{R_1 + R_2}. \tag{5}$$

It seems that, in general, $\left|S_x^{\omega_0}\right| \leqslant 0.5$, $\left|S_x^Q\right| < 1$ where x stands for any active or passive circuit parameter. For a temperature-stabilized filter using an operational amplifier with GB specified at certain supply voltages, the above sensitivities can be considered low.

The circuit was constructed in the laboratory using an internally compensated operational amplifier $(A \simeq GB/s)$, type LM741 (National Semiconductor Corporation), having 935 kHz unity gain crossover frequency at 15 V power supplies. The following 10 percent tolerance components were used:

$$R_1 = 120 \text{ k}\Omega, \quad R_2 = 120 \text{ k}\Omega, \quad C = 1 \text{ nF}.$$

In Fig. 2 the experimental results are shown to agree with the theoretical computer-calculated plot.

By taking V_3 instead of V_2 as the output, i.e.,

$$\frac{V_3}{V_1} = \frac{s^2 CR_1R_2}{s^2 CR_1R_2 + s(R_1 + R_2) + R_1 \cdot GB}, \tag{6}$$

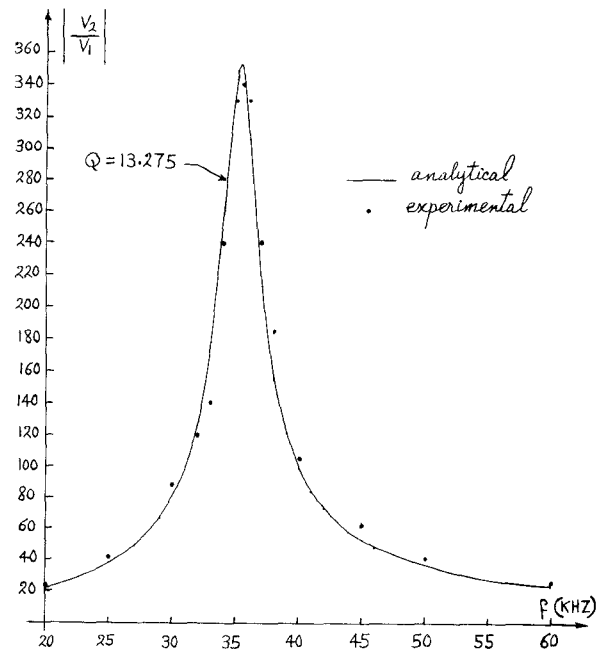the same circuit may be used as a high-pass filter whose practi-

Fig. 2. Bandpass characteristics.

cal utility is limited unless the output is followed by an ideal voltage follower.

REFERENCES

[1] A. Budak and D. M. Petrela, "Frequency limitations of active filters using operational amplifiers," *IEEE Trans. Circuit Theory*, vol. CT-19, pp. 322–328, July 1972.
[2] K. R. Rao and S. Srinivasan, "A bandpass filter using the operational amplifier pole," *IEEE J. Solid-State Circuits*, pp. 245–246, June 1973.

An Integrated Illumination-to-Frequency Converter

S. T. LEUNG AND HARRY H. L. KWOK

Abstract—A simple integrated illumination-to-frequency converter has been fabricated following the field-effect modified transistor (FEMT) as suggested by Nordstrom and Meindl. We have made a careful analysis of the performance of the device and have found that no external photodiode is needed for the device to operate properly. An external capacitor, connected across the external base to collector junction, can significantly extend the range of operation of the device as a light detector.

I. INTRODUCTION

We wish to report the fabrication of a fully integrated illumination-to-frequency converter. The converter has been fabricated similar to the field-effect modified transistor (FEMT) reported by Nordstrom and Meindl [1], [2]. However, the present device uses the external base–collector junction as a photodiode and is capable of achieving illumination-to-frequency conversion for a wide range of illumination with no additional external circuitry. The dynamic range of the